Design of a Compact Wideband Antenna Array for Microwave Imaging Applications

Jan PUSKELY, Tomáš MIKULÁŠEK, Zbyněk RAIDA

Dept. of Radio Electronics, Brno University of Technology, Purkyňova 118, 612 00 Brno, Czech Republic

puskely@feec.vutbr.cz, xmikul30@stud.feec.vutbr.cz, raida@feec.vutbr.cz

Abstract. *In the paper, wideband antenna arrays aimed at microwave imaging applications and SAR applications operating at K_a band were designed. The antenna array feeding network is realized by a low-loss SIW technology. Moreover, we have replaced the large feed network comprised of various T and Y junctions by a simple broadband network of compact size to more reduce losses in the substrate integrated waveguide and also save space on the PCB. The designed power 8-way divider is complemented by a wideband substrate integrated waveguide to a grounded coplanar waveguide transition and directly connected to the antenna elements. The measured results of antenna array are consistent with our simulation. Obtained results of the developed array demonstrated improvement compared to previously developed binary feed networks with microstrip or SIW splitters.*

Keywords

Vivaldi antenna, Yagi antenna, microwave imaging, SIW feeding network, SAR, K_a frequency band.

1. Introduction

Recently, the microwave imaging systems have attracted many researchers. Their fields of application are different included medical imaging [1]-[3], detection of buried objects [4]. [5], non destructive testing or evaluation [5], [6], and tracking [7]. For these systems, high-gain antennas with a relatively wide bandwidth for high resolution are designed. Almost constant radiation pattern, good input match and low insertion loss over a desired frequency range are in addition equally important requirements [8], [9].

There are a variety of UWB antennas; nevertheless, in the paper we study the antipodal Vivaldi antenna and the planar Yagi antenna having good potential for applications that require broadband characteristics [7], [10], [11]. These antennas have a high gain, a wide bandwidth, high efficiency and a compact structure. Thanks to small lateral dimensions, both elements can form an array, which is suitable for imaging applications. The design of a relatively

simple feeding network with low insertion loss for such an array is a big challenge [7], [12].

A relatively high loss can be observed when the antenna array is fed by a microstrip feeding structure [7]. Due to the advantages of the substrate integrated waveguide (SIW) technology (low cost, high Q-factor, low insertion loss), the feeding network implemented by SIW is widely used to reduce the insertion loss of the feeding network at higher frequencies especially [8], [12]-[15].

All the published feeding networks are based on the binary architecture, which is composed of seven (in the case of a 1x8 array) T-junctions (Y-junctions). Unfortunately, these T-junctions add losses to the final insertion loss. Further, the area of the printed circuit board (PCB), which is occupied by the feeding network, is several times larger compared to the area occupied by antennas [12].
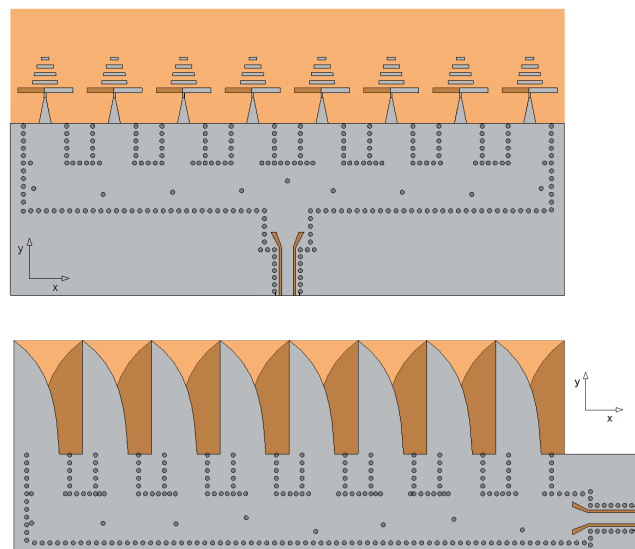
Fig. 1. The proposed structures of the antenna arrays; top: symmetrical feeding network with Yagi antennas; bottom: unsymmetrical feeding network with Vivladi antennas.

Our goal is to realize the antenna system that will lead to reasonable imaging capabilities operating in K_a band. In the paper, we introduce the developed millimeter wave compact antenna array fed by the SIW feeding network. In our design, we replaced the large feeding network by

a simple relatively broadband network of a compact size (see Fig. 1). The designed feeding network reduces the losses in SIW feeds and represents an elegant solution saving space on the PCB. The network is fed by a wideband transition SIW to a grounded coplanar waveguide (GCPW) to obtain good impedance matching [14]. The antenna element and the low loss SIW feeding network represented by the power 8-way divider are discussed in detail below.

2. Antenna Array Configuration

We have designed a relatively broadband high-gain antenna array for microwave image applications, SAR applications and radar systems. We analyzed two antenna elements and two versions of feeding structures, shown in Fig. 1, for this purpose. The arrays comprise of the antenna elements, a SIW 8-way power divider and a transition SIW to GCPW. The arrays are designed on the substrate of thickness of 0.508 mm and permittivity 2.2. The implemented SIW has via holes with a diameter of 0.5 mm and the space between via holes is 0.9 mm.

The array gain and radiation patterns are functions of the elements' spacing and differential phase between its elements. Increasing the spacing between the elements reduces the mutual coupling effect. On the other hand, it enlarges the size of the array and may cause the appearance of grating lobes near the high-frequency end of the band. Fig. 2 shows the simulated gain of both arrays as a function of the inter element spacing. It is also clear that the element spacing beyond a wavelength generates grating lobes. The optimum spacing is about 0.9λ, where a maximum gain can be obtained. Finally, the array elements spacing was chosen 0.87λ (at ~32.5 GHz) to obtain an in-phase feeding for each element, almost maximum directivity and in addition to decrease the antenna size. The overall size of arrays is 24.2 mm × 71 mm and 30.2 mm × 60 mm, respectively.
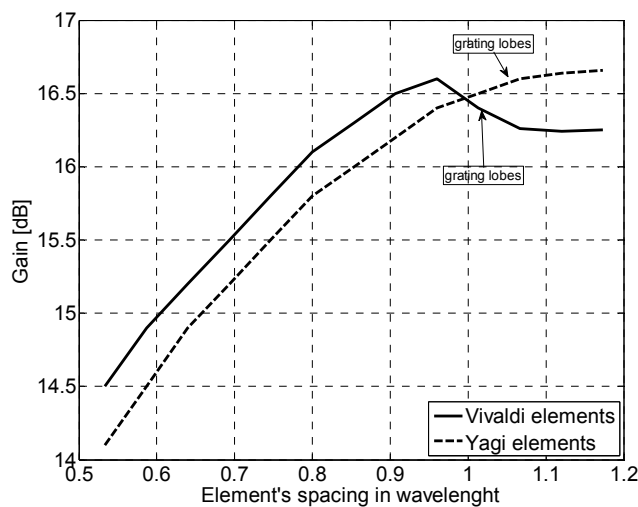

Fig. 2. Simulated gain of eight-element arrays vs. the elements' spacing.

2.1 Antenna Elements

In this section, we will study the Vivaldi antenna and the printed Yagi antenna [10], [11]. Both have potential for applications requiring broadband characteristics. These antennas have been optimized from a radiation pattern and impedance matching view point over a desired frequency range.

A. Vivaldi antenna

A single-element of Vivaldi antenna used in arrays is shown in Fig. 3 (left). The width of Vivaldi antenna $W_a = 8$ mm is given by spacing of the elements and the width of SIW feed $W_{siw} = 5$ mm is given by the cutoff frequency of the equivalent waveguide. The optimized variables of the single antenna element were the antenna length L_a, the offset of arms dA and the parameters M, N of the exponential taper profile defined by the function

$$y = \pm M \cdot \exp(N \cdot x). \qquad (1)$$

After optimization, the resulting final values are as follows: $L_a = 13.2$ mm, $dA = 2.7$ mm, $M = 0.200$ and $N = 0.251$.
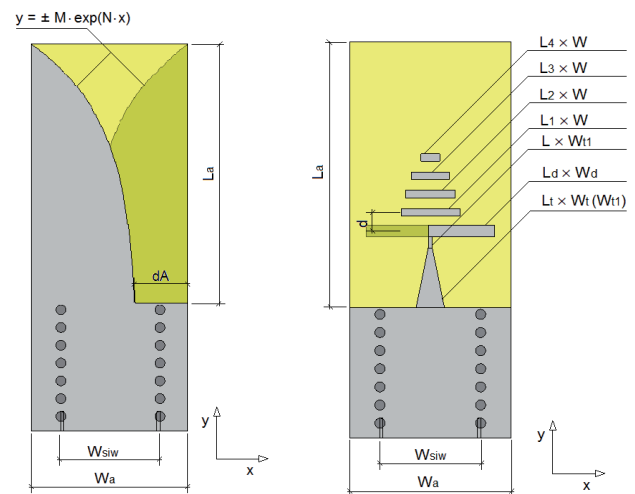

Fig. 3. The proposed antenna elements of the antenna array.

The simulated reflection coefficients $|s_{11}|$ and mutual couplings between two elements are shown in Fig. 4 and Fig. 5, respectively. The impedance matching is better than 10 dB and mutual coupling is lower than -20 dB in the whole K_a band. The radiation patterns of a single Vivaldi element are depicted in Fig. 6. Gain reaches of about 7 dBi.

B. Printed Yagi antenna

The geometry of the proposed Yagi antenna fed by the SIW is shown in Fig. 3 (right). The structure is made of a driving dipole and 4 directors printed on the top layer of the substrate. The top and bottom ground planes act as a reflector element for the antenna. The driving dipole (L_d, W_d) and the balun (L_t, W_t, L, W_{tl}) are built on both sides of the substrate. The impedance matching and antenna gain

were optimized by changing the width and length of the driver element and directors (L_{1-4}, W) and the spacing between the directors and driver element (d). The optimized dimensions of the antenna element are the following (in mm): $W_t = 1.40$, $W_{t1} = 0.20$, $W_d = 0.56$, $W = 0.37$, $L_t = 2.95$, $L = 0.55$, $L_d = 3.27$, $L_1 = 2.91$, $L_2 = 2.48$, $L_3 = 1.91$, $L_4 = 0.93$ and $d = 0.90$. The choice of dimensions W_a and W_{siw} was mentioned above.

The simulated reflection coefficient $|s_{11}|$ of the printed Yagi antenna element is depicted in Fig. 4 and is under -10 dB with an impedance bandwidth as wide as 13 GHz (~25 GHz to 38 GHz). The mutual coupling is lower than -25 dB in the whole K_a band, see Fig. 5. The radiation patterns of the Yagi element are depicted in Fig. 7. The gain is comparable to the Vivaldi antenna and is about 7 dBi too.
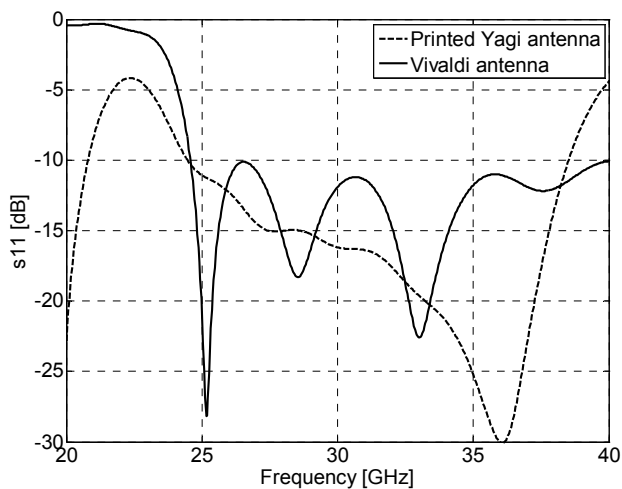

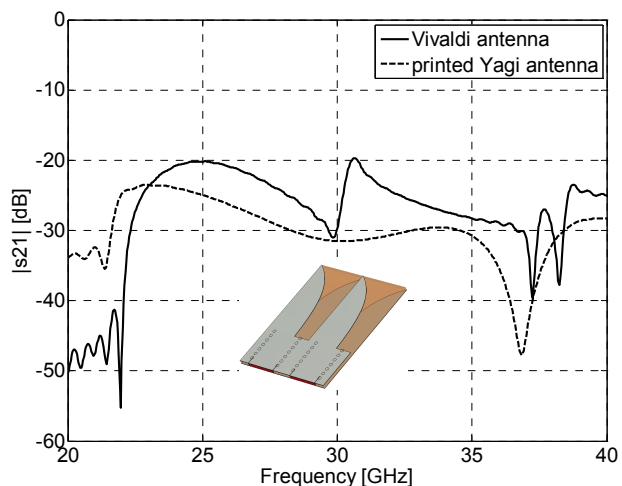**Fig. 4.** Reflection coefficients $|s_{11}|$ of analyzed antenna elements.

Fig. 5. Mutual coupling $|s_{21}|$ between two elements of each analyzed antenna.

The Yagi antenna is matched better than the Vivaldi antenna in the 25–38 GHz band and also the mutual coupling between two elements is lower. On the other hand, radiation patterns of the Vivaldi antenna are more directional and therefore more suitable for building array from

the resolution view point. Nevertheless, the choice of antenna element will depend on the resulting gain and impedance matching of the final array.
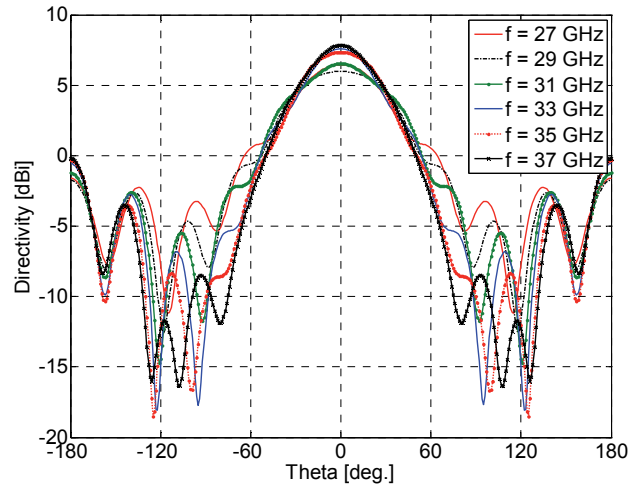

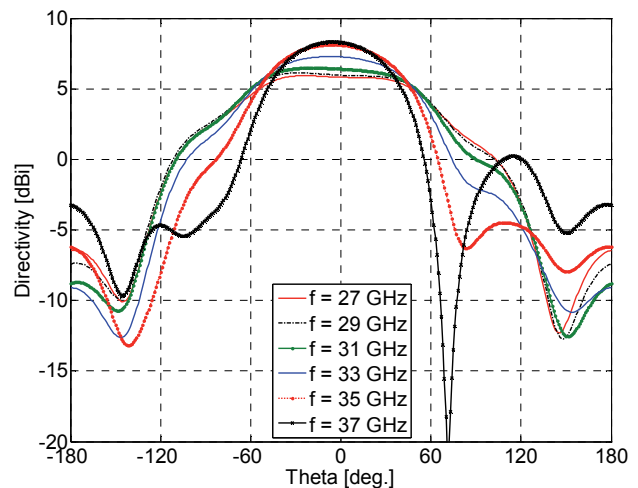**Fig. 6.** Radiation patterns of Vivaldi antenna element.

Fig. 7. Radiation patterns of Yagi antenna element.

2.2 Design of a SIW 8-way Power Divider

The design of a low loss and wideband SIW 8-way divider replacing the conventional binary feeding network is the most important step. First, we analyzed the phase balance of both feeding structures (Fig. 1) in the basic configuration, i.e. without the tuning via holes.

Simulation results of dividers without tuning pins show that the phase balance is narrowband and significantly influences the radiation patterns. The unsymmetrical version of the divider causes main beam deflection $\pm 8°$ in the given band due to reflections of the unbalanced phase. Whereas, the symmetrical version of the divider produces significant grating lobes, which appear in patterns at border frequencies of the operation band due to reflections of the unbalanced phase and amplitude distribution.

In order to force this type of SIW feeding network to divide the power in such a way to obtain an almost con-

stant radiation pattern over the operation band, we have to add tuning vias to both networks, as shown in Fig. 8 and Fig. 11, and optimize their positions. Positions of vias Cx affect the impedance matching and positions of vias Px influence the phase and the amplitude of each antenna element. Optimization was set to meet the following goals in the maximum possible band:

- Pure in-phase feeding which produces a radiation pattern perpendicular to the antenna plane;

- Such an amplitude distribution which does not cause noticeable side lobes;

- Low insertion loss of the feeding network and good impedance matching.
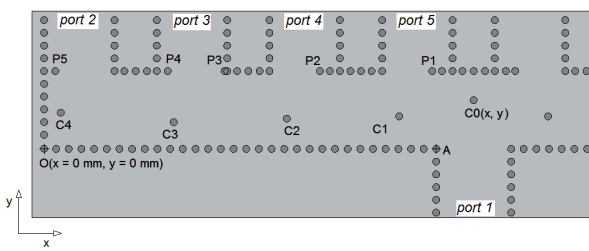
A. Symmetrical feeding network

Firstly, we analyzed a symmetrical feeding structure. The optimization tasks were the grating lobes and impedance matching. In order to suppress side lobes, we computed amplitude distribution according to Dolph-Chebyshev to have a suppression of more than 20 dB in the desired band [16]. Finally, the chosen distribution corresponds to a suppression of 25 dB according to Tab. 1.

| Element number	-30dB	-25 dB	-20 dB
1	1.000	1.000	1.000
2	0.810	0.842	0.873
3	0.517	0.584	0.657
4	0.261	0.377	0.577

Tab. 1. Feeding weights by Dolph-Chebyshev for 8 elements.

The positions of vias Cx and Px in the coordinate system obtained by Particle Swarm Optimization are the following according to Fig. 8 (in mm): $C0(x = 30.5, y = 3.44)$, $C1(25.21, 2.31)$, $C2(17.24, 2.14)$, $C3(9.2, 1.89)$, $C4(1.19, 2.56)$, $P1(27.55, 5.5)$, $P2(19.58, 5.5)$, $P3(12.82, 5.5)$, $P4(8.78, 5.5)$, $P5(0.79, 0.55)$ and $A(27.84, 0)$.
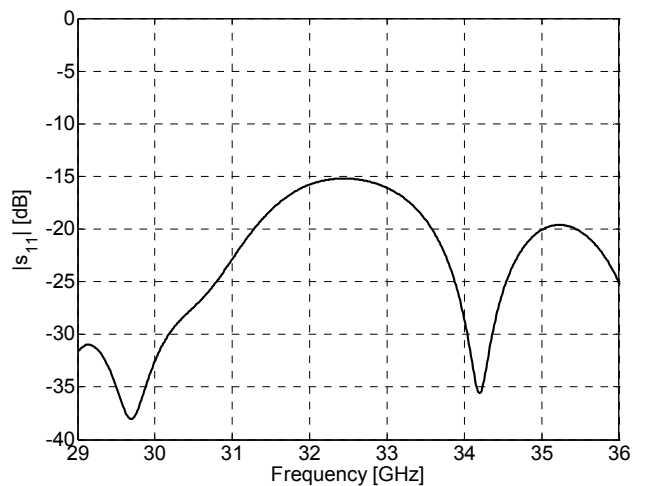
Fig. 8. Optimized feeding structure of symmetrical version.

The results of the optimized feeding network are depicted in Fig. 9 and Fig. 10. The reflection coefficients of the divider are less than -15 dB in the desired frequency band. Radiation patterns are shown in Fig. 17. Although, the amplitude and phase distributions of the proposed divider, shown in Fig. 9, are not designed to provide a balanced power division over a wide band, the antenna gain of 14.5 dB is sustained over the 4 GHz bandwidth. The side lobes level does not exceed -20 dB over the range 31 GHz to 34 GHz. The insertion losses of each branch are obvious from the amplitude balance of the divider, see Fig. 9.
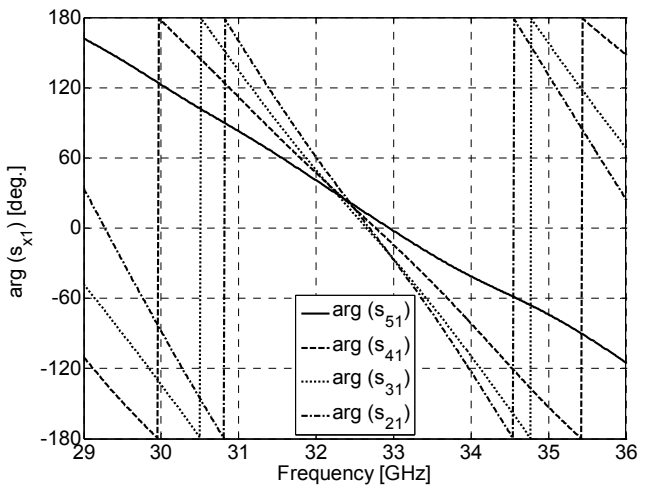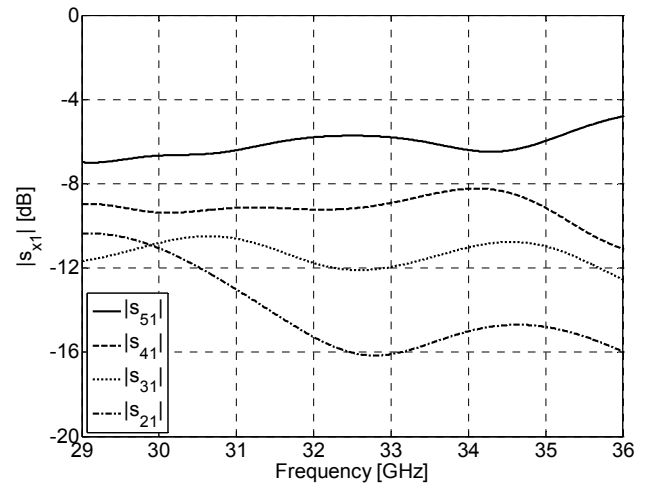
Fig. 9. Amplitude and phase balance of the symmetrical feeding structure.

Fig. 10. Impedance matching of the symmetrical feeding structure.

B. Unsymmetrical feeding network

In the case of unsymmetrical feeding network (Fig. 11), the main optimization task was to design such a phase distribution that produces a radiation pattern perpendicular to the antenna plane in the operating band.

Other tasks were impedance matching and low side lobe levels.

During the analysis we tried different optimization strategies to fulfill the criteria. Optimized reflection coefficients were good but the amplitude and phase balance of the proposed divider were always similar to the results presented in Fig. 12. As obvious from the dependency of the radiation pattern on frequency, the unbalance phase distribution deflects the main beam in the desired band. The deflection range is almost 32° over the 30.5 GHz to 37.0 GHz frequency band, see Fig. 13.

Thus, the antenna structure could provide applications in radar systems [17] in which space can be scanned by frequency sweeping in a 32° angular range in our case.
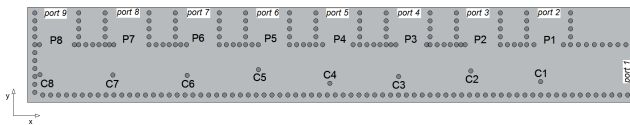

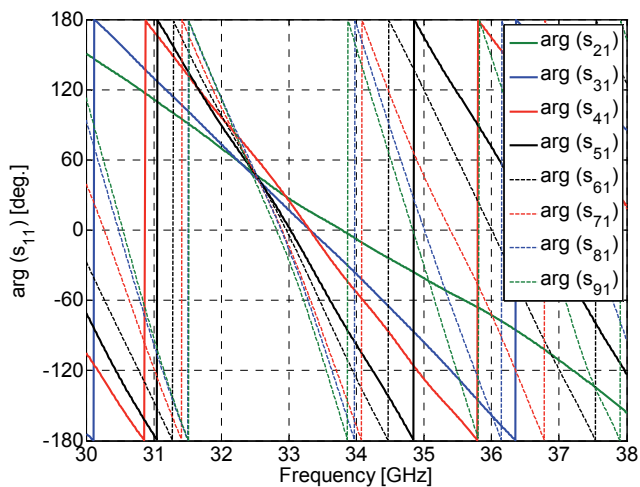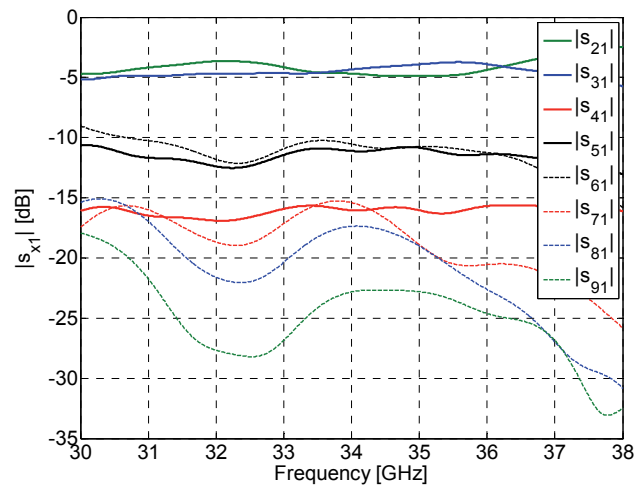**Fig. 11.** Optimized feeding structure of unsymmetrical version.

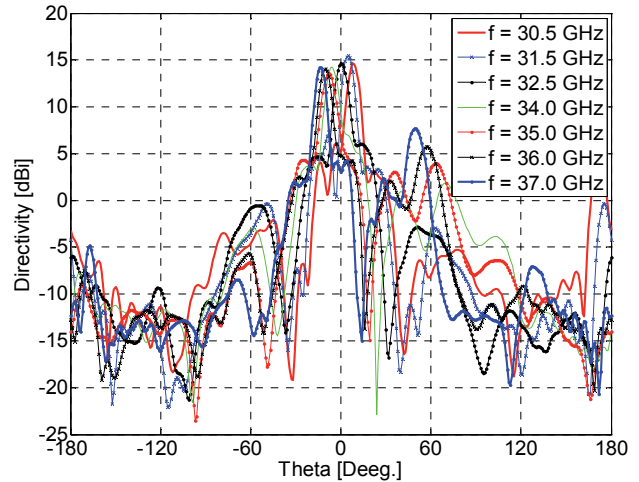**Fig. 12.** Amplitude and phase balance of the unsymmetrical feeding structure.

Fig. 13. The dependency of the radiation pattern on the frequency of the antenna array with an unsymmetrical feeding network.

2.3 Design of Transition SIW to GCPW

The power divider was complemented by a transition SIW to GCPW which is more appropriate for our purpose than the transition SIW into microstrip line through simple tapering. The wideband transition is achieved by using a tapered coupling slot [14] as shown in Fig. 14. The dimensions of transition are the following (in mm): $w_{siw} = 1.5$; $w_{lin} = 0.65$; $w_{sl1} = 0.3$; $w_{sl2} = 0.6$; $l_{t1} = 6$; $l_{t2} = 1.8$.
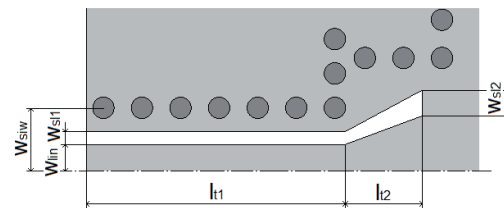

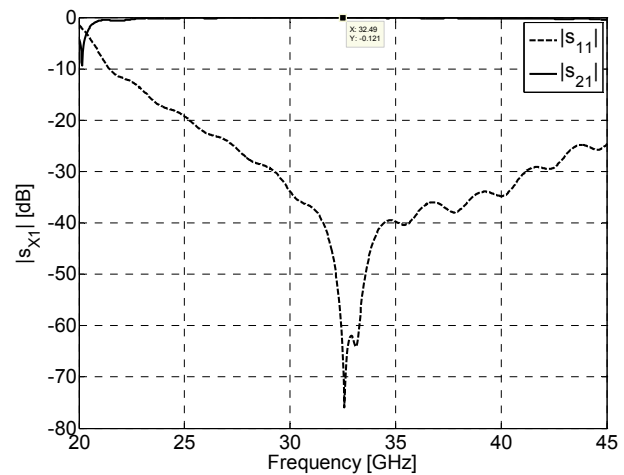**Fig. 14.** Half of the designed SIW to GCPW transition.

Fig. 15. Simulated return loss and insertion loss of the proposed SIW-GCPW transition.

Figure 15 displays the simulated results of the transitions. It can be observed that the return loss is better than -20 dB and insertion loss is lower than -0.2 dB over the K_a frequency band.

3. Designed Antenna Array

The simulated results of complete antenna arrays with a symmetrical version of the feeding network complemented by a grounded coplanar transition, but with different antenna elements, are presented in this part.

Simulated reflection coefficients $|s_{11}|$ of both antenna arrays are shown in Fig. 16. Obviously, both arrays are matched well and have a similar bandwidth. From the radiation point of view, the Vivaldi antenna array has a constant radiation pattern in the wider bandwidth (about 3 GHz) compared to the printed Yagi antenna array when the obtained bandwidth is about 2 GHz, see Fig. 17 and Fig. 18.
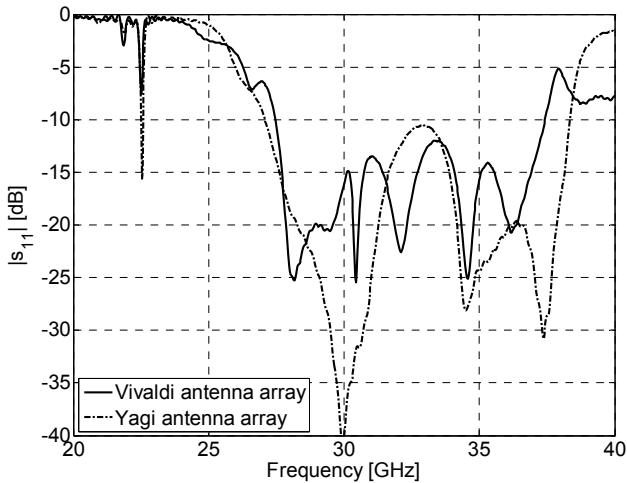

Fig. 16. Comparison of simulated return loss of the Vivaldi and Yagi antenna.

Frequency [GHz]	30.0	30.5	31.0	32.5	34.0	34.5	35.0
Gain [dB]	7.7	14.3	15.7	16.0	15.5	14.7	11.3
SLL, E-plane [dB]	-4.0	-4.9	-19.6	-21.4	-20.0	-6.6	-8.7
Front to Back ratio [dB]	9.4	10.3	19.6	21.1	20.1	18.4	16.1
Efficiency [%]	88.8	89.4	91.4	92.0	91.0	90.9	90.4

Tab. 2. Simulated radiation properties of the Vivaldi antenna array

The Vivaldi antenna arrays were complemented by a grounded coplanar launch connector. The simulated reflection coefficients $|s_{11}|$ of the antenna array with connector are shown in Fig. 21. The influence of the connector is noticeable but matching is still better than 10 dB over the working band. The simulated radiation patterns are shown in Fig. 22 and Fig. 23. They indicate low side lobe levels which do not exceed -20 dB in E-plane over the range from

31 GHz to 34 GHz. Antenna gain is around 15 dB in that band. Radiation parameters are summarized in Tab. 2.

E-field distribution of the Vivaldi antenna array at the center frequency is shown in Fig. 19. It shows ideal in-phase feeding and distribution of the input power into each branch.
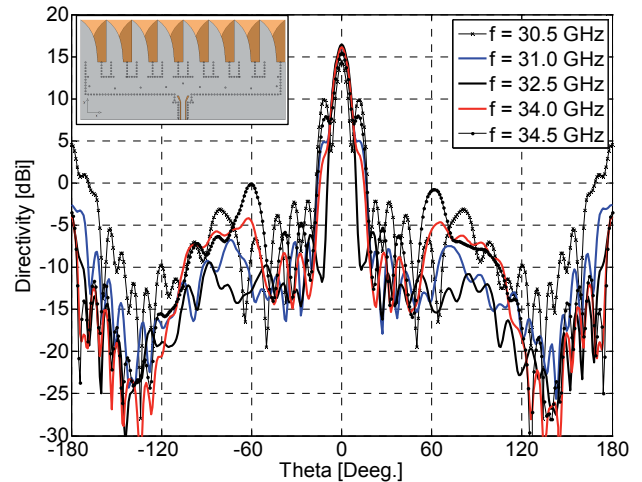

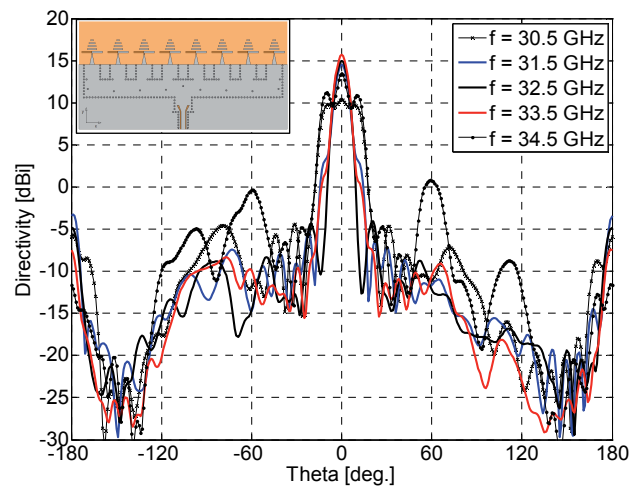**Fig. 17.** Simulated radiation patterns of the Vivaldi antenna; E-plane.

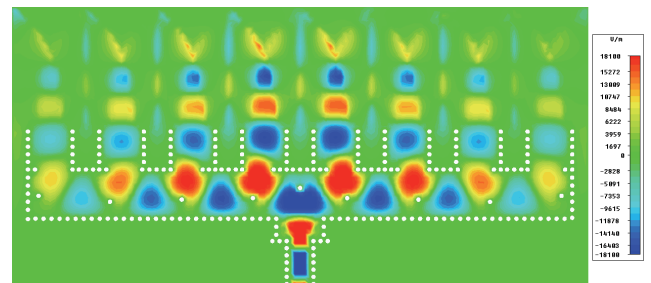**Fig. 18.** Simulated radiation patterns of the Yagi antenna; E-plane.

Fig. 19. E-field distribution of the Vivaldi antenna array; f = 32.5 GHz.

4. Prototyped Vivaldi Antenna Array and Experimental Results

The Vivaldi antenna array was designed and fabricated to operate with desired radiation properties over the 31 GHz to 34 GHz frequency range. It was printed on a 0.508 mm thick substrate with a dielectric constant of 2.2 and a loss tangent of 0.0009. The fabricated Vivaldi antenna array is shown Fig. 20.
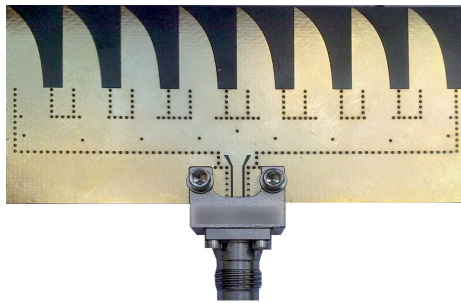

Fig. 20. Fabricated Vivaldi antenna array.

The measured reflection coefficients $|s_{11}|$ are shown in Fig. 21 and are in good agreement with simulation. The impedance matching of the array is, except for a small part, better than 10 dB over almost 11 GHz bandwidth (34%).
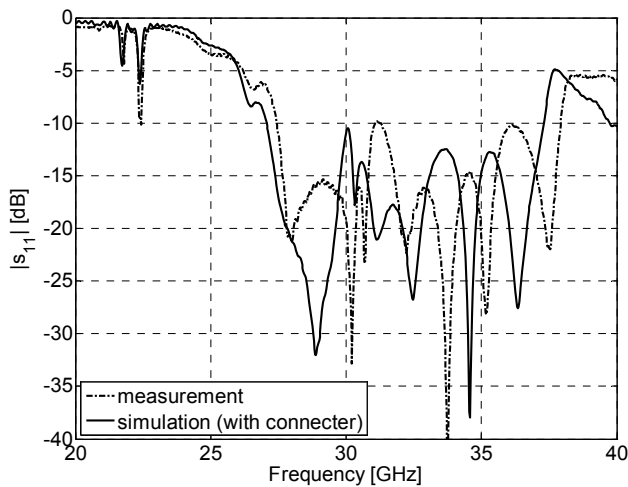

Fig. 21. Reflection coefficient of the Vivaldi array with/without connector.

Frequency [GHz]	31.0	32.5	34.0
Gain [dB]	14.4	15.0	14.1
SLL, E-plane [dB]	-20.6	-22.6	-20.0
Main lobe width E-cut [°]	8.9	9.0	8.7
Front to Back ration [dB]	34.1	29.8	26.7
Cross-polarization level [dB]	-13.8	-17.6	-15.4

Tab. 3. Measured radiation properties of the Vivaldi antenna array.

Figure 22 and 23 show the measured E-plane and H-plane radiation patterns of the antenna at 31 GHz, 32.5 GHz and 34 GHz. Good agreement can be observed between simulation and measurements. The gain was

measured as 14.1-15.0 dB and SLL was below -20 dB across the entire bandwidth. In addition, the front-to-back ratio is found to be better than 27 dB and the cross-polarization level is better than -14 dB across the entire bandwidth. Measured radiation parameters are summarized in Tab. 3.
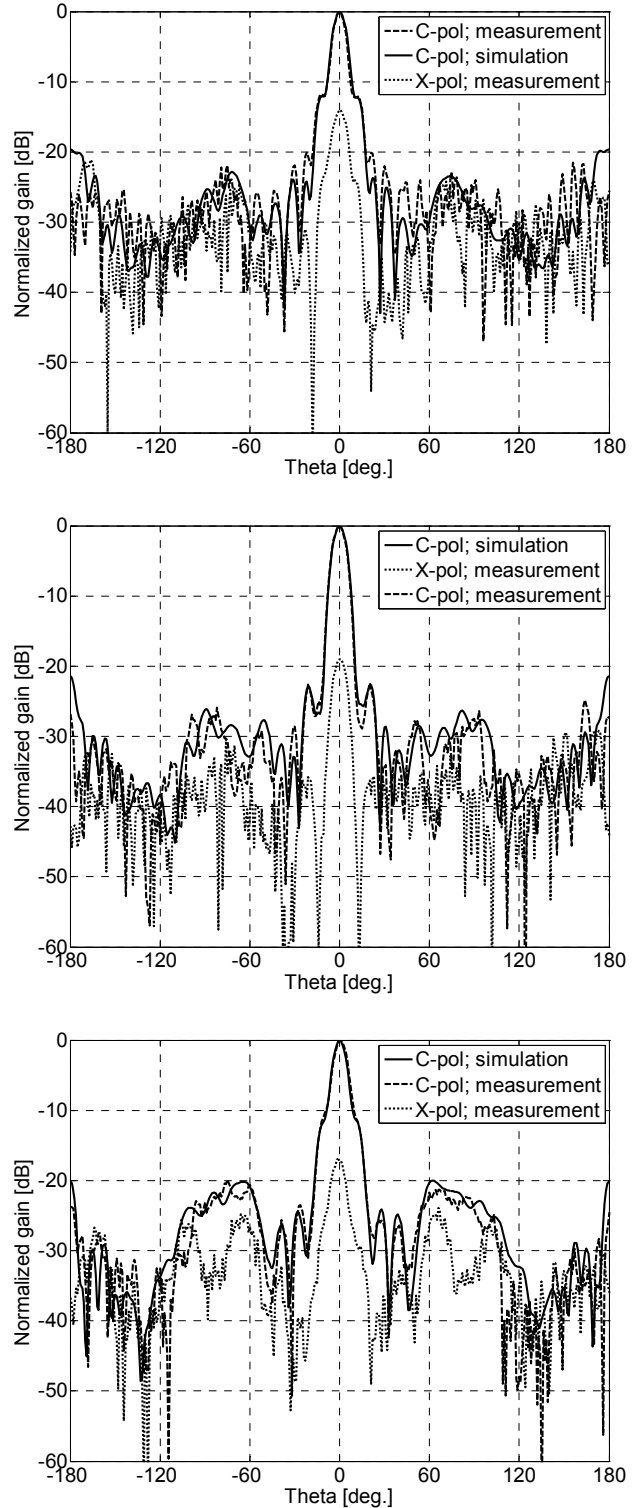

Fig. 22. E-plane of radiation patterns of the Vivaldi array; from top to bottom: 31 GHz, 32.5 GHz and 34 GHz .
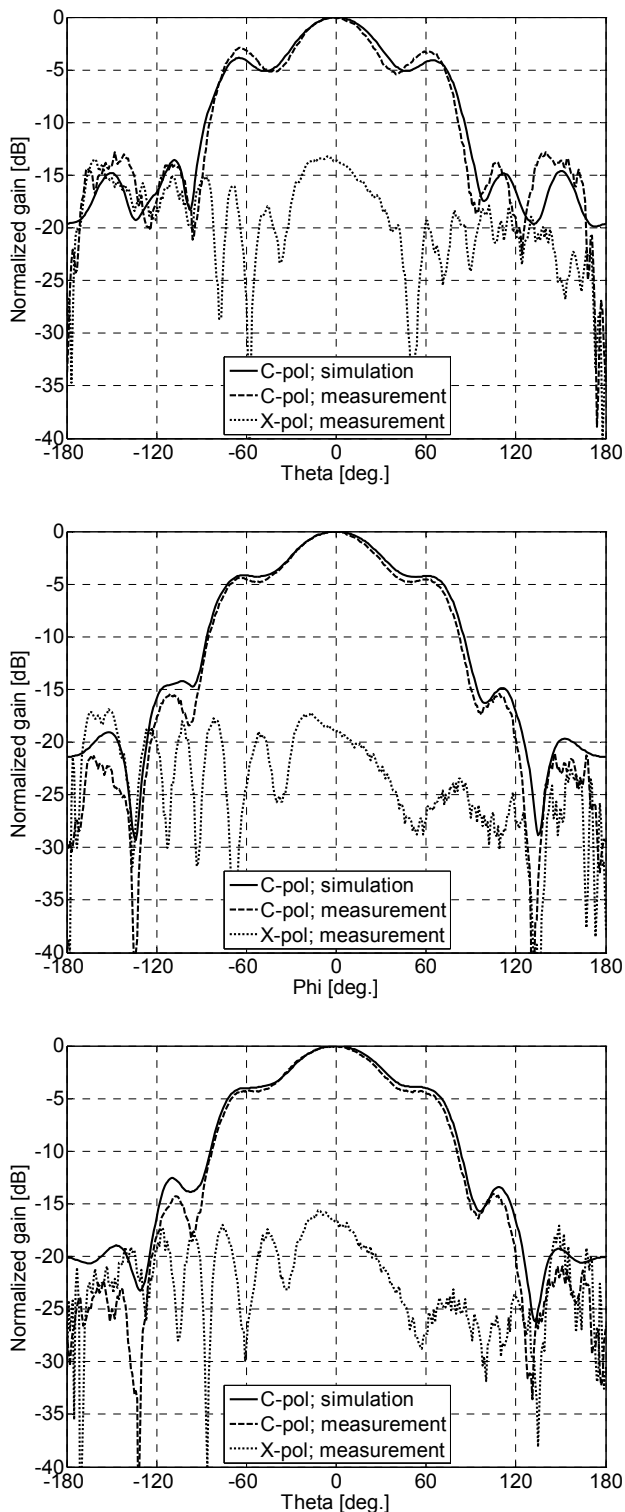
Fig. 23. H-plane of radiation patterns of the Vivaldi array; from top to bottom: 31 GHz, 32.5 GHz and 34GHz.

5. Conclusions

In the paper, we developed a millimeter wave compact antenna array aimed at microwave image applications operating at K_a band. In our design, we replaced the conventional binary feeding network by a compact size 8-way power divider using SIW technology and complemented it with a wideband SIW to GCPW transition to minimize the insertion loss. Further, we analyzed two antenna elements to be able to cover the whole K_a band. Finally, the antipodal Vivaldi antenna, as a basic element of the array, was chosen.

The designed Vivaldi antenna array was fabricated and validated by measurements. From the impedance matching view point, the achieved bandwidth was almost 34% (27-38 GHz). But if the array should operate with desired radiation properties then the bandwidth is narrower by about 10% (31-34 GHz). The developed Vivaldi antenna array achieved high gain, narrow beam width in the E-plane and sufficient side lobe suppression. Further, the measured front-to-back ratio was found to be better than 25 dB and the cross-polarization level is better than -14 dB across the entire bandwidth.

The future extensions of this research will be in designing of SIW feeding network for building the larger antenna arrays of 8x8 elements.

Acknowledgements

References

[1] FEAR, E. C., LI, X., HAGNESS, S. C., STUCHLY, M. A. Confocal microwave imaging for breast cancer detection: localization of tumors in three dimensions. *IEEE Transactions on Biomedical Engineering*, Aug. 2002, vol. 49, no. 8, p. 812-822.

[2] BOND, E. J., LI, X., HAGNESS, S. C., VAN VEEN, B. D. Microwave imaging via space-time beamforming for early detection of breast cancer. *IEEE Transactions on Antennas and Propagation*, Aug. 2003, vol. 51, no. 8, p.1690-1705.

[3] SIEGEL, P. H. Terahertz technology in biology and medicine. *IEEE Transactions on Microwave Theory and Techniques*, Oct. 2004, vol. 52, no. 10, p. 2438-2447.

[4] BERMANI, E., BONI, A., CAORSI, S., MASSA, A. An innovative real-time technique for buried object detection. *IEEE Trans. Geosci. Remote Sens.*, 2003, vol. 41, no. 4, p. 927-931.

[5] PASTORINO, M. Stochastic optimization methods applied to microwave imaging: A review. *IEEE Transactions on Antennas and Propagation*, March 2007, vol. 55, no. 3, p. 538-548.

[6] HUI, X., TAO, L., YANSHAN, S. The application research of microwave imaging in nondestructive testing of concrete wall. In

The Sixth World Congress on Intelligent Control and Automation WCICA 2006. 2006, vol. 1, p. 5157-5161.

[7] YANG, Y., WANG, Y., FATHY, A. E. Design of compact Vivaldi antenna arrays for UWB see through wall applications. *Progress in Electromagnetics Research* PIER 82, 2008, p. 401-418.

[8] KAZEMI, R., FATHY, A. E., SADEGHZADEH, R. A. Dielectric rod antenna array with substrate integrated waveguide planar feed network for wideband applications. *IEEE Transactions on Antennas and Propagation,* March 2012, vol. 60, no. 3, p. 1312-1319.

[9] LAZARO, A., GIRBAU, D., VILLARINO, R. Simulated and experimental investigation of microwave imaging using UWB. *Progress in Electromagnetics Research*, 2009, vol. 94, p. 263-280.

[10] LIN, S., YANG, S., FATHY, A. E., ELSHERBINI, A. Development of a novel UWB Vivaldi antenna array using SIW technology. *Progress in Electromagnetics Research*, 2009, vol. 90, p. 369-384.

[11] ZHANG, Z., WU, K., YANG, N. Broadband millimeter-wave quasi-Yagi antenna using Substrate Integrated Waveguide technique. In *IEEE Radio and Wireless Symposium 2008*, Jan. 2008, p. 671-674.

[12] HAO, Z., HONG, W., LI, H., ZHANG, H., WU, K. Multiway broadband substrate integrated waveguide (SIW) power divider. In *IEEE Ant. Propag. Soc. Int. Symp.*, 2005, p. 639-642.

[13] LI BIN, DONG LIANG, ZHANG JIAO-CHENG. The research of broadband millimeter-wave Vivaldi array antenna using SIW technique. In *International Conference ICMMT 2010*. 2010, p. 997-1000.

[14] SONGNAN, Y., ELSHERBINI, A., LIN, S., FATHY, A. E., KAMEL, A., ELHENNAWY, H. A highly efficient Vivaldi antenna array design on thick substrate and fed by SIW structure with integrated GCPW feed. In *Antennas and Propagation Society International Symposium 2007*. 2007, p. 1985-1988.

[15] YANG, Y., ZHANG, C., LIN, S., FATHY, A. E. Development of an ultra wideband Vivaldi antenna array. In *IEEE Antennas and Propagation Society International Symposium 2005*. 2005, p. 606 to 609.

[16] DOLPH, L. C. The current distribution of broadside arrays with optimized the relationship between beamwidth and side-lobe level. *Proc. IRE and Waves and Electrons*, June 1946.

[17] ALVAREZ-LOPEZ, Y., GARCIA-GONZALEZ, C., VAZQUEZ-ANTUNA, C., VER-HOEYE, S., LAS HERAS ANDRES, F. Frequency scanning based radar system. *Progress in Electromagnetics Research*, 2012, vol. 132, p. 275-296.

About Authors ...

Jan PUSKELY was born in Přerov, the Czech Republic, in 1982. He received his master's degree in 2007 and his Ph.D. degree in 2011, both in Electrical Engineering from the Brno University of Technology. At present, he is with the Department of Radio Electronics, Brno University of Technology, as a researcher. His research interest is focused on measurements in the near field of antennas and design of antennas.

Tomáš MIKULÁŠEK was born in the Czech Republic in 1985. He received his master's degree from the Faculty of Electrical Engineering and Communication (FEEC), Brno University of Technology (BUT), Czech Republic, in 2009. At the present, he is a PhD student at the Dept. of Radio Electronics FEEC BUT.

Zbyněk RAIDA received Ing. (M.Sc.) and Dr. (Ph.D.) degrees from the Brno University of Technology in 1991 and 1994, respectively. Since 1993, he has been with the Dept. of Radio Electronics, FEEC BUT as an assistant professor (1993 to 1998), associate professor (1999 to 2003), and professor (since 2004). In 1997, he spent six months at the Laboratoire de Hyperfrequences, Universite Catholique de Louvain, Belgium working on variational methods of numerical analysis of electromagnetic structures. Since 2006, he has been the head of the Dept. of Radio Electronics. Zbyněk Raida has been working together with his students and colleagues on numerical modeling and optimization of electromagnetic structures, exploitation of artificial neural networks for solving electromagnetic compatibility issues, and the design of special antennas. Prof. Raida is a member of the IEEE Microwave Theory and Techniques Society.